BIOLOGICAL APPLICATIONS OF RAMAN SPECTROSCOPY

VOLUME 2: Resonance Raman Spectra of Polyenes and Aromatics

Edited by

THOMAS G. SPIRO

Department of Chemistry
Princeton University

A WILEY-INTERSCIENCE PUBLICATION

JOHN WILEY & SONS

NEW YORK CHICHESTER BRISBANE
TORONTO SINGAPORE

Library of Congress Cataloging in Publication Data:

Resonance Raman spectra of polyenes and aromatics.
(Biological applications of Raman spectroscopy; v. 2)
"A Wiley-Interscience publication."
Includes bibliographies and index.
1. Biomolecules—Spectra. 2. Aromatic compounds—Spectra. 3. Polyenes—Spectra. 4. Raman spectroscopy.
I. Spiro, Thomas G., 1935- . II. Series.
QP519.9.R36B56 vol. 2 574.19'285 s 86-24757
ISBN 0-471-81574-8 [574.19'285]

Printed in the United States of America

10 9 8 7 6 5 4 3 2 1

Contributors

PAUL R. CAREY, Division of Biological Sciences, National Research Council of Canada, Ottawa, Ontario, Canada

AKIKO Y. HIRAKAWA, Faculty of Pharmaceutical Sciences, University of Tokyo, Hongo, Bungyo-ku, Tokyo, Japan

BRUCE S. HUDSON, Department of Chemistry and Institute of Molecular Biology, University of Oregon, Eugene, Oregon

RICHARD A. MATHIES, Department of Chemistry, University of California, Berkeley, California

LELAND C. MAYNE, Department of Chemistry and Institute of Molecular Biology, University of Oregon, Eugene, Oregon

JAMES T. MCFARLAND, Department of Chemistry, University of Wisconsin, Milwaukee, Wisconsin

ANNE B. MYERS, Department of Chemistry, University of California, Berkeley, California

YOSHIFUMA NISHIMURA, Faculty of Pharmaceutical Sciences, University of Tokyo, Hongo, Bungyo-ku, Tokyo, Japan

ILONA PALINGS, Department of Chemistry, University of California, Berkeley, California

WARNER PETICOLAS, Department of Chemistry and Institute of Molecular Biology, University of Oregon, Eugene, Oregon

STEVEN O. SMITH, Department of Chemistry, University of California, Berkeley, California

MASAMICHI TSUBOI, Faculty of Pharmaceutical Sciences, University of Tokyo, Hongo, Bungyo-ku, Tokyo, Japan

Preface

Some 60 years have passed since the discovery by C. V. Raman (1) of the effect that bears his name. In the decade following this discovery, Raman spectroscopy provided data on the vibrational frequencies of many molecules (2). Only during the 1940s did the introduction of practical infrared (IR) spectrometers lead to the displacement of the more laborious Raman method for routine recording of vibrational spectra. In the prelaser days, heroic measures had to be taken to record the very weak spectra emanating from the Raman effect; this generally involved the placement of a large optically clear sample inside a high-intensity discharge lamp (3). The concentration of light power provided by the laser has revolutionized Raman technology (4) and vastly increased its applicability.

Biological molecules have historically been problematic as an arena for vibrational spectroscopy, despite the promise of this method as a probe of molecular structure. Infrared spectroscopy is constrained by the fact that water, the ubiquitous solvent of biology, is a strong absorber of IR radiation. It is a weak Raman scatterer, and, as early as 1938, J. T. Edsall expressed the cautious hope that Raman spectroscopy could be applied to the study of proteins (5). Twenty years elapsed before this hope was rewarded with a "quite faint" photographic Raman spectrum of lysozyme (6). The first laser Raman spectra of proteins were published in 1968 (7). Since then the growth of the literature on biological applications of Raman spectroscopy has been explosive.

This set of three volumes provides a comprehensive view of a still new and rapidly evolving field through summaries of representative areas by authorities in biological Raman applications. A major research objective

has been to extract information from Raman spectra about the conformations of biological macromolecules: proteins, nucleic acids, and lipids. This is the theme of Volume 1, which considers these macromolecules in isolation and also in organized biological assemblies: ocular lenses, viruses, and membranes. In addition, the collective vibrational modes of macromolecules are considered from a theoretical standpoint, and there is a review of the promising new area of vibrational optical activity.

The introduction of the laser actually had two revolutionary influences on Raman spectroscopy. One was the dramatic relaxation of constraints on the size and optical clarity of the sample and the attendant improvement in signal quality. The other was the ability to produce Raman scattering from absorbing samples, thanks to the minimization of the light path allowed by the directional laser beam. This permitted systematic studies of the resonance Raman effect, which has been an extremely active and productive area from both experimental and theoretical perspectives. The importance of the resonance Raman effect for biological applications is that it can provide dramatically increased sensitivity and selectivity. The theory of the effect is presented in Volume 2, which also explores applications to rhodopsin, to the purine and pyrimidine bases of nucleic acids, to the peptide backbone and chromophoric side chains of proteins, to flavins, and, finally, to the introduction of resonance Raman labels into biological systems. Heme proteins have provided a particularly rich opportunity for resonance Raman studies, and various aspects of work in this area are discussed in Volume 3, which also includes applications to chlorophylls and nonheme metalloproteins.

It is hoped that these volumes give a sense of the high promise that Raman spectroscopy holds for providing unique and important molecular information in biology. They are dedicated to Professor Richard C. Lord, who, perhaps more than any other single individual, has been responsible for the development of this realm of science. His pioneering studies on proteins and nucleic acids have been an inspiration to most current practitioners in the field, and the students that he trained have played an important role in pushing back its frontiers. He is held in the highest esteem by his many friends and admirers, who respond to his wisdom and to his wonderful human qualities. One of his former students, Professor George Thomas, has written the Dedication that appears in Volume 1.

THOMAS G. SPIRO

Princeton, New Jersey
January 1987

REFERENCES

1. C. V. Raman and K. S. Krishnan, *Nature,* **121**, I (1928).
2. J. H. Hibben, *The Raman Effect and Its Chemical Applications,* Reinhold, New York, 1939.
3. G. R. Harrison, R. C. Lord, and J. R. Loofbourow, *Practical Spectroscopy,* Prentice-Hall, Englewood Cliffs, New Jersey, Chap. 18, 1948.
4. S. P. S. Porto and D. L. Wood, *J. Opt. Soc. Am.*, **52**, 251 (1962).
5. J. T. Edsall, *Cold Spring Harbor Symp. Quant. Biol.*, **6**, 440–449 (1938).
6. D. Garfinkle and J. T. Edsall, *J. Am. Chem. Soc.*, **80**, 3818–3823 (1958).
7. M. C. Tobin, *Science,* **161**, 68 (1968).

Contents

1

Resonance Raman Intensities: A Probe of Excited-State Structure and Dynamics

ANNE B. MYERS
RICHARD A. MATHIES

Department of Chemistry
University of California
Berkeley, California

Contents

1 INTRODUCTION

Resonance Raman scattering is a versatile spectroscopic technique for studying the structure of biological molecules. The resonance condition arises when the wavelength used to excite the Raman scattering falls within an electronic absorption band, causing the vibrations of the absorbing species to be selectively enhanced. This makes it possible to obtain the vibrational spectrum of a colored prosthetic group in a protein without interference from the vibrations of the amino acid environment. The vibrational frequencies provide detailed information about the geometry and electronic structure of the chromophore in its ground state. In addition, the *intensities* of the Raman lines tell us about the symmetry, equilibrium geometry, and dynamics of the resonant excited electronic state. Many biological chromophores exhibit diffuse electronic absorption spectra that provide little information about the specific structural changes that occur on excitation; furthermore, the most interesting excited states are often those that are short-lived as a result of rapid photochemistry or energy transfer, making direct time-resolved studies of the excited state difficult. For these reasons, resonance Raman may be the most direct way to explore excited-state structure in many biological systems, as well as in other molecules for which vibrationally resolved spectra cannot be obtained. The intensity of each resonance Raman line reflects the projection of the excited-state geometry change onto a specific ground-state normal coordinate, thus providing detailed information about the excited state with the resolution of a ground-state vibrational spectrum. For example, Figure 1 shows that excitation into the unstructured visible absorption band of bacteriorhodopsin generates a Raman spectrum exhibiting well-resolved vibrational lines. How can we analyze these intensities to learn more about the excited-state structure and dynamics of bacteriorhodopsin?

The relationship between resonance Raman intensities and excited-state structure has been known since the early work of Tang and Albrecht (1) (see Refs. 2–6 for recent reviews). However, there have been comparatively few attempts to use experimental Raman intensities to deduce excited-state properties quantitatively. This is partly because the theoretical description of resonance Raman scattering appears quite complex, and even at the simplest level of approximation there is generally no direct

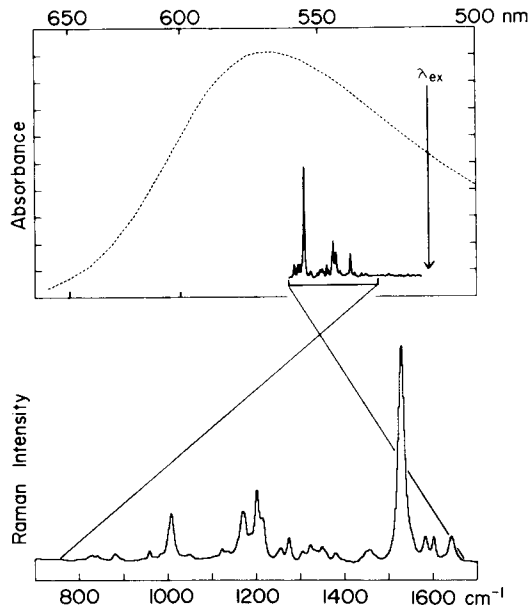

Figure 1. Absorption and resonance Raman spectra of bacteriorhodopsin. Determination of the excited-state structure of the retinal prosthetic group in bacteriorhodopsin will help us to understand how light absorption drives transmembrane proton pumping. Unfortunately, the diffuse absorption spectrum provides little information about excited-state structure. However, the frequencies and intensities of the individual vibronic lines that make up this band can be obtained from the resonance Raman spectrum because the intensities of the well-resolved Raman lines depend on the projection of the excited-state geometry change onto the ground-state normal modes.

relationship between the intensities in a single Raman spectrum and the excited-state parameters of interest. Also, although methods for computing resonance Raman intensities from a given set of potential surfaces have been discussed in detail, rather less attention has been given to methods for working backward from intensities to potential surfaces. This is the problem faced by the experimentalist interested in analyzing Raman intensities in polyatomic molecules for which reliable calculated potential surfaces are not available.

The traditional approach to evaluating the resonance Raman cross section involves summation over all the vibrational levels of the resonant electronic state. Unfortunately, this procedure can be computationally intractable for large molecules undergoing large excited-state geometry changes. Alternative time-dependent theories of Raman scattering developed by Hizhnyakov and Tehver (7) and by Heller (8–10) alleviate the computational difficulties often encountered with the sum-over states.

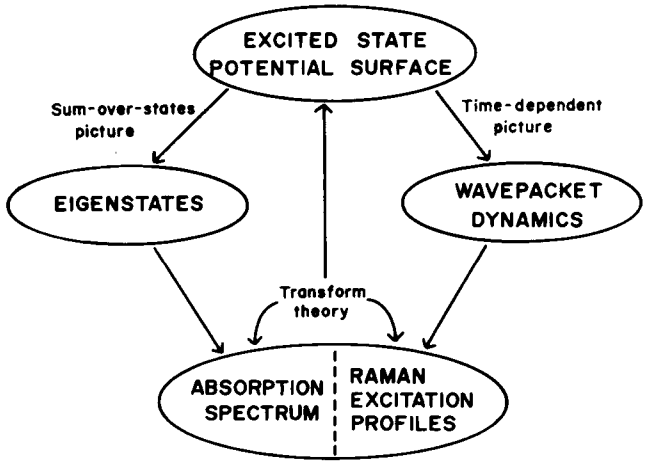

Figure 2. The relationship between the sum-over-states, time-dependent, and transform approaches for analyzing resonance Raman intensities and absorption spectra.

Many of these same computational advantages are shared by a third class of theoretical approaches, the transform methods (7,11–13), which are particularly well suited for going directly from experimental data to an excited-state structure. One principal goal of this chapter is to clarify the relationship between these three theoretical approaches (see Figure 2) and to compare the advantages and disadvantages of each.

We begin by presenting the theory of resonance Raman intensities from these three theoretical viewpoints. In addition, we have explicitly tabulated the formulas required to implement each computational method at the simplest levels of approximation appropriate for large molecules. The next section briefly discusses the experimental measurement of both relative and absolute Raman intensities on resonance. Specific methods for extracting excited-state parameters from experimental intensities and converting the dimensionless normal coordinate displacements to actual geometry changes are then presented and illustrated with applications to bacteriorhodopsin and stilbene. We conclude with a summary and a brief discussion of prospects for the future.

2 THEORY OF RESONANCE RAMAN INTENSITIES

2.1 Sum-Over-States Picture

The traditional approach to resonance Raman intensities begins with the dispersion expressions originally derived by Kramers and Heisenberg

(14) and Dirac (15) from second-order time-dependent perturbation theory. The total radiated power resulting from a Raman transition from state $|I\rangle$ to state $|F\rangle$, integrated over all directions and polarizations of scattered light and assuming a randomly oriented sample, is given by (16)

$$P_{I\to F} = I\sigma_{I\to F}(E_L) \tag{1}$$

where

$$\sigma_{I\to F}(E_L) = \frac{8\pi e^4 E_s^3 E_L}{9\hbar^4 c^4} \sum_{\rho,\lambda} |(\alpha_{\rho\lambda})_{I\to F}|^2 \tag{2}$$

and

$$(\alpha_{\rho\lambda})_{I\to F} = \sum_V \frac{\langle F|m_\rho|V\rangle\langle V|m_\lambda|I\rangle}{E_V - E_I - E_L - i\Gamma} + \frac{\langle F|m_\lambda|V\rangle\langle V|m_\rho|I\rangle}{E_V - E_F + E_L - i\Gamma} \tag{3}$$

In Eqs. (2) and (3), E_L and E_s are the incident and scattered photon energies; $|I\rangle$, $|V\rangle$, and $|F\rangle$ are the initial, intermediate, and final vibronic states and E_I, E_V, and E_F are their energies; Γ is the homogeneous linewidth; and m_ρ is a vector component of the transition dipole length operator. In Eq. (2), σ has units of a cross section (area), $P_{I\to F}$ is the radiated power in photons per second, and I is the incident photon flux (photons area^{-1} sec^{-1}). If $P_{I\to F}$ and I are defined in terms of *energy* rather than *photons,* the $E_s^3 E_L$ factor in Eq. (2) is changed to E_s^4 (17). The definition of the cross section in terms of photons is more convenient for comparison with experiments performed by use of photon-counting detection and is used throughout.

The interpretation of Eqs. (1)–(3) is that Raman scattering is a two-photon process involving virtual absorption from the initial state to the entire manifold of excited vibronic states, followed by virtual emission to the final state. The "nonresonant" second term in Eq. (3) arises from the case where emission precedes absorption. Since no measurement of the state of the system is made during the intermediate time, contributions from all intermediate states are summed at the amplitude level before squaring. The magnitude of the contribution from each state depends on both the transition length and the energy denominator. As the energy of the incident radiation approaches resonance with a particular electronic state, vibronic levels of that state begin to dominate the sum.

When the excitation wavelength falls within a single, strongly allowed absorption band, several approximations are usually made to simplify Eqs. (2) and (3). First, the Born–Oppenheimer approximation is invoked to

factor the vibronic states into products of electronic and vibrational states. The dipole length matrix elements in Eq. (3) then become, for example,

$$\langle F|m_\rho|V\rangle = \langle f|\langle g|m_\rho|e\rangle|v\rangle = \langle f|M_\rho(Q)|v\rangle \tag{4}$$

where $|g\rangle$ and $|e\rangle$ are the ground and excited electronic states, respectively, and $|f\rangle$ and $|v\rangle$ are vibrational levels of these electronic states. The electronic transition length matrix element $M_\rho(Q)$ is a function of the nuclear coordinates Q because the Born–Oppenheimer electronic states depend parametrically on the nuclear coordinates. However, this nuclear coordinate dependence is usually neglected when on resonance with a strongly allowed electronic transition—that is, $M_\rho(Q)$ is replaced by $M_\rho(Q_0)$, where Q_0 is the ground-state equilibrium geometry. This is the Condon approximation, and it amounts to assuming that the magnitude of the transition length evaluated at Q_0 is much larger than the *variation* of M over the range of Q sampled by the initial and final ground-state vibrational wavefunctions. Non-Condon effects are discussed briefly in Section 2.1.4. Finally, only the vibrational levels of the resonant electronic state are considered to make an important contribution to the sum over virtual states, and the nonresonant terms are dropped. Now that only one excited electronic state is involved, a set of axes can be chosen such that only one of the elements of the transition length vector is nonzero, and the sum over the ρ and λ indices can be eliminated.

The expression for the resonance Raman polarizability now becomes

$$\alpha_{i\to f}(E_L) = M^2 \sum_v \frac{\langle f|v\rangle\langle v|i\rangle}{\varepsilon_v - \varepsilon_i + E_0 - E_L - i\Gamma} \tag{5}$$

where the zero–zero energy E_0 is the energy separation between the lowest vibrational levels of the ground and excited electronic states (see Figure 3), and ε_v and ε_i are the energies of the vibrational states $|v\rangle$ and $|i\rangle$. This is the Albrecht A-term expression for excitation within an allowed absorption band (16). The complete expression for the resonance Raman cross section, with the constants in Eq. (2) evaluated, becomes

$$\sigma_{i\to f} = 5.87 \times 10^{-19} M^4 E_s^3 E_L \left| \sum_v \frac{\langle f|v\rangle\langle v|i\rangle}{\varepsilon_v - \varepsilon_i + E_0 - E_L - i\Gamma} \right|^2 \tag{6}$$

with E_L, E_s, E_0, ε_i, ε_v, and Γ in cm^{-1}; M in angstroms (Å), and σ in $Å^2$/molecule.

For comparison, the optical absorption cross section at the same level of approximation is given by (5)

$$\sigma_A(E_L) = \frac{4\pi^2 e^2 M^2 E_L}{3\hbar cn} \sum_v \frac{\Gamma}{\pi} \frac{|\langle v|i\rangle|^2}{(\varepsilon_v - \varepsilon_i + E_0 - E_L)^2 + \Gamma^2} \tag{7}$$

where n is the solution refractive index (see Section 2.1.6) and σ (Å^2/molecule) is related to the molar absorptivity ε (M^{-1} cm^{-1}) by

$$\sigma = 2.303 \times 10^{19} \frac{\varepsilon}{N_A} \tag{8}$$

where N_A is Avogadro's number. Evaluation of the constants in Eq. (7) gives a prefactor of $3.05 \times 10^{-2} M^2 E_L \Gamma / n$.

The absorption cross section depends on the same excited-state parameters as does the Raman cross section. Although the absorption spectrum is often too diffuse to provide much specific information, it can be measured very accurately, and the excited-state parameters used to fit the Raman intensities should always be required to fit the absorption as well. Note that the absorption and Raman cross sections depend differently on the homogeneous linewidth. In absorption, each term in the sum over states involves a *normalized* Lorentzian lineshape. Increasing Γ broadens the spectrum but does not change the integrated intensity. In contrast, by writing the Raman amplitude as a sum of real and imaginary terms

$$\alpha_{i\to f} = M^2 \sum_v \frac{\langle f|v\rangle\langle v|i\rangle}{(\varepsilon_v - \varepsilon_i + E_0 - E_L)^2 + \Gamma^2} [(\varepsilon_v - \varepsilon_i + E_0 - E_L) + i\Gamma] \tag{9}$$

it can be seen that the imaginary part is also a normalized Lorentzian, but the real part of the scattering amplitude always becomes smaller with increasing Γ. Thus, if enough is known about the rest of the system, *absolute* resonance Raman cross sections can be used to determine Γ (9,18,19).

If calculated potential surfaces were available, it would be possible, in principle, to solve for the full multidimensional eigenstates of the excited-state surface and then evaluate Eqs. (6) and (7) exactly. However, the Raman intensities would then depend on the entire potential surface, and if the calculated intensities did not agree with the experimental ones, it would be very difficult to ascertain which aspects of the calculated surface were at fault. When working with large molecules, it appears preferable to begin at the simplest reasonable level of approximation, where the Raman intensities depend on only a small number of parameters that can be determined from the data in a straightforward way. If this modeling is unsuccessful, selective relaxation of approximations may help to identify the dominant additional effects.

2.1.1 Multidimensional Separable Harmonic Approximation. The simplest approach to evaluating the multidimensional Franck–Condon factors in Eqs. (6) and (7) is to assume that the ground- and excited-state potential surfaces are harmonic and differ only in their equilibrium positions. The vibrational frequencies and normal coordinates are then identical in the ground and excited states, and a system of N vibrational modes can be treated as a collection of N independent pairs of harmonic oscillators as shown in Figure 3. Each degree of freedom is completely described by a frequency ω and an origin shift Δ in dimensionless normal coordinates. The dimensionless coordinate q is related to the Cartesian coordinate x by $q = (\mu\omega/\hbar)^{1/2}x$, where μ is the reduced mass and ω is the frequency in hertz.

The multidimensional Franck–Condon factors can now be written as simple products of one-dimensional overlaps; for example,

$$\langle f|v\rangle = \prod_{j=1}^{N} \langle f_j|v_j\rangle \tag{10}$$

Equations (5) and (7) for fundamental Raman scattering and absorption can now be written more explicitly as follows:

$$\alpha_{i\to i+1} = M^2 \sum_{v_1}\sum_{v_2}\cdots\sum_{v_N} \frac{\langle (i+1)_1|v_1\rangle\langle v_1|i_1\rangle\Pi_{j=2}^{N}\langle i_j|v_j\rangle\langle v_j|i_j\rangle}{\Sigma_{j=1}^{N}\hbar\omega_j(v_j - i_j) + E_0 - E_L - i\Gamma} \tag{11}$$

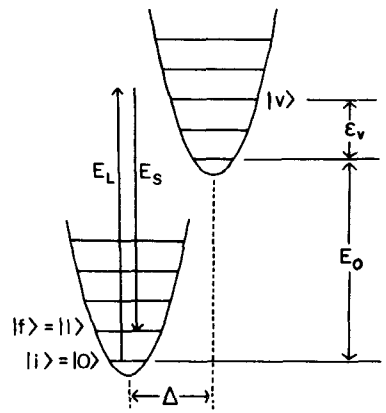

Figure 3. Resonance Raman scattering in a separable harmonic system. Each vibrational degree of freedom is treated as a pair of ground- and excited-state harmonic surfaces with frequency ω, displaced by an amount Δ. The system is excited by incident light of energy E_L from state $|i\rangle$ to the set of virtual levels ($|v\rangle$); it then returns to level $|f\rangle$, emitting a photon of energy E_s. In fundamental scattering, $|f\rangle$ differs from $|i\rangle$ by only one quantum of excitation in one vibrational mode.